Lorenzo Mariti
Department of Mechanical and Aerospace Engineering,
West Virginia University,
Morgantown, WV 26506
e-mail: mariti@ing.uniroma2.it

Victor H. Mucino
Professor
Department of Mechanical and Aerospace Engineering,
West Virginia University,
Morgantown, WV 26506
e-mail: victor.mucino@mail.wvu.edu

Ettore Pennestrí
Professor
Department of Industrial Engineering,
University of Rome "Tor Vergata",
Rome, Italy
e-mail: pennestri@mec.uniroma2.it

Andres Cavezza
Department of Mechanical and Aerospace Engineering,
West Virginia University,
Morgantown, WV 25606
e-mail: acavezza@mix.wvu.edu

Mridul Gautam
Professor
Department of Mechanical and Aerospace Engineering,
West Virginia University,
Morgantown, WV 26506
e-mail: mgautam@mail.wvu.edu

Pier Paolo Valentini
Assistant Professor
Department of Industrial Engineering,
University of Rome "Tor Vergata",
Rome, Italy
e-mail: valentini@ing.uniroma2.it

Optimization of a High-Speed Deployment Slider–Crank Mechanism: A Design Charts Approach

Mechanical and aerospace applications often require that mechanisms deploy in a quick stable and reliable way. The objective of this study is to implement a general optimization procedure to perform a first stage conceptual design of HSD mechanisms, focusing on both kinematics and dynamics. In particular, the authors will focus on the development of design charts. In the very first part of the work, a parametric lumped-mass system will be modeled in order to reduce the number of parameters for the synthesis phase. A correlation will be established between geometry, inertia and initial position to guarantee the maximum value of acceleration during deployment of the deployable arm by means of the principle of virtual work. In the second part of this work, the influence of important factors such as friction and joint clearance on the overall dynamics of the system will be investigated. Finally, a coupled dynamic and structural analysis of the helical spring, that actuates the mechanism, will be carried out in order to achieve optimal performance. The developed charts will also take into account the space limitation requirement, that are often needed for both aerospace and mechanical applications. A final example will summarize all the points covered by this research effort. Results will be validated using the commercial software ABAQUS. [DOI: 10.1115/1.4025702]

1 Introduction

The dynamics of mechanical and aerospace systems is often addressed by considering that bodies are operating at reasonably low speeds. However, high inertial loads caused by high speed deployment (HSD), directly affect the dynamics and the structural behavior of the system, influencing both its reliability and stability. The use of spring actuated high speed mechanism (HSM) may be essential in agricultural, aerospace, military and ballistic applications in which some objects have to quickly deploy for different purposes. They may be also needed in mechanical applications, for the deployment of roll-over protective structures for safety purposes in automotive and agricultural tractors applications. Often, very high precision is imperative in the deployment phase. For this reason the design and prototyping phases play a fundamental role in the product development chain.

During all design steps, the designer has to take into account different issues, which can significantly affect the actual behavior of the mechanical system.

One issue addressed in this paper is the modeling of the kinematic joints. When high links speeds and high value of the constraint reaction forces are considered, it may be useful to model the joints taking into account friction and clearance and investigating on how they affect the overall dynamics of the system.

Published literature has focused on the dynamic analysis of deployment structures, but only few of them place specific attention on the HSDM problem. Mitsugi et al. [1] developed a model for the deployment mechanism of a large space antenna, but they only considered small deployment velocities. Dietz et al. [2] developed a similar work on the deployment of a solar array using SimPack. Rossoni et al. [3] gave the guideline for the design of the deployment mechanism for the ST5 mission, but they still focused on small deployment speed. Wallrapp and Wiedemann [4] studied the deployment of a flexible solar array using modal techniques, but they limited their investigation to the case of small speed. Contribution related to high speed deployment mechanism applied to the deployment of safety structures can be found in Refs. [5–7]. In these application, the authors focused on a conceptual design demonstration without searching for a general methodology. In the first part of this paper, a lumped mass model of the mechanism will be implemented and a correlation between the inertia parameter, the geometry of the

Contributed by the Mechanisms and Robotics Committee of ASME for publication in the JOURNAL OF MECHANICAL DESIGN. Manuscript received July 5, 2012; final manuscript received September 15, 2013; published online April 28, 2014. Assoc. Editor: Oscar Altuzarra.

mechanism and the initial con which guarantees the minimum deployment time will be established.

Similarly many contributions on dynamics formulation for the real joints description in flexible multibody dynamics are on the record. In 1998, Ravn [8] proposed a study on local dry contact between planar rigid bodies, in which a set of contact forces is computed according to Hertz model. In 2004, Flores et al. [9] proposed a 2D revolute clearance joint model with friction and lubrication. They modeled a revolute joint with clearance using an equivalent force element, taking into account free motion, contact, and damping. Some other papers presented methodologies to implement the 3D kinematics and dynamics of joints. In Ref. [10], Valentini et al. proposed a modeling of hydrodynamic journal bearing in spatial multibody systems, in which both rotational and squeeze effects together with tilting effect have been taken into account. One year later, Valentini et al. [11] discussed a methodology based on a kinematic approach using the dual-algebra fundamentals to simulate the presence of joint with clearance in generic multibody systems. This methodology has been applied to an industrial case of an automotive transmission of a Cardan coupling. In Ref. [12], Valentini et al. studied a model of revolute joint with friction and clearance suitable for general multibody applications.

In this paper, the influence of friction on the dynamics of HSD is investigated. In order to maintain a lumped model, a simple planar model has been considered in order to simulate the dynamics of the mechanism.

The HSD motion needs to be activated by the use of a spring actuator. There could be several ways to obtain such action. In this paper, the authors have focused on the optimum design of a helical spring actuator, taking into account both dynamics and structural issues. Substantial body of published literature exists on helical springs dynamic and structural behavior. Lee et al. [13] proposed an efficient method for the computation of a coil spring stiffness for low frequencies. Johnson [14] proposed the equations for an optimum design of an high frequency operating helical spring, considering both structural failure constraints and dynamic effects. Yildrim [15] used the transfer matrix method to investigate the parameters which affect the free vibration frequency of helical springs. Starting from the results of the dynamic model (e.g., deployment time), the idea is to design the optimum spring on the basis of natural frequency, maximum shear failure theory, and space limitation requirements.

The *design charts approach* has been used several times for the kinematic synthesis of mechanisms. Freudenstein [16] used this approach searching for the dimensions of a plane crank–and–rocker linkage, or drag linkage, with prescribed values of the maximum and minimum angular velocity ratios of the cranks. Dukkipati et al. [17] extended the previous approach to the three dimensional case of a slider–crank. Again Freudenstein [18] used the design charts approach for the determination of minimum and maximum velocities and accelerations of general four-link mechanisms. However, in all these studies, the authors considered the kinematics of the problem without taking into account the mass distribution and the external forces acting on the system. Moreover, they searched for a stationary point of the velocity, which means null value of the acceleration. The main element of novelty of this work is the addition of the mass distribution and the external forces within the models of kinematic synthesis previously mentioned. In our procedure, the configurations with the maximum values of accelerations can be found through a *dynamic synthesis* process. No previous optimization processes of HSD mechanisms based on the development of design charts are known to the authors. The procedure developed and presented herein sets the basis for a general optimization tool for HSD mechanisms. In fact, the algorithms herein proposed can be easily extended to other deployment devices, filling a gap in technical literature.

2 Dynamic Model Setup

In this section, the model setup will be presented and the simplifying hypotheses discussed. First, the concentrated-mass model will be described and then the theoretical background behind the friction modeling at the revolute joints and the spring dynamic model will be discussed. Figure 1 shows a schematic representation of the slider–crank mechanism under analysis.

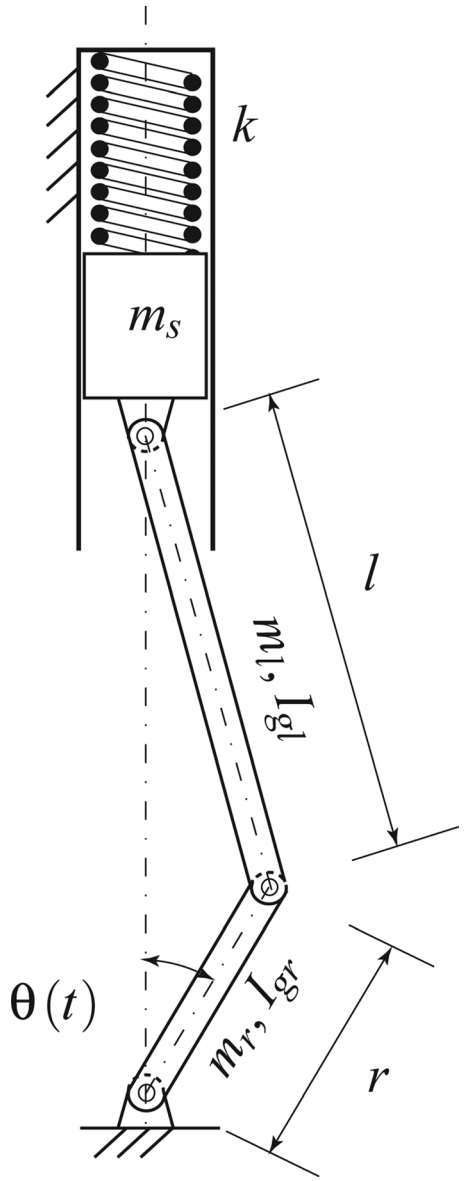

Fig. 1 Scheme of the Slider–Crank mechanism under analysis

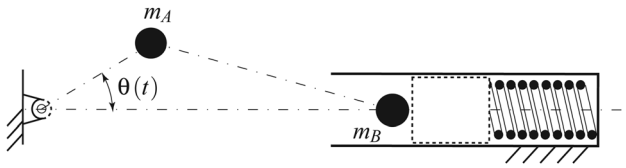

Fig. 2 Lumped mass model

2.1. The Lumped Mass Model. In order to reduce the number of parameters for the development of design charts, the first step is to create a lumped-mass model of the mechanism. For this purpose, the criteria proposed by Wittenbauer [19] were adopted. In particular, the overall inertia of the system has been distributed into two masses, as shown in Fig. 2.

After algebraic manipulations on the equations presented in Ref. [19], the values of the two masses can be computed according to the following equations:

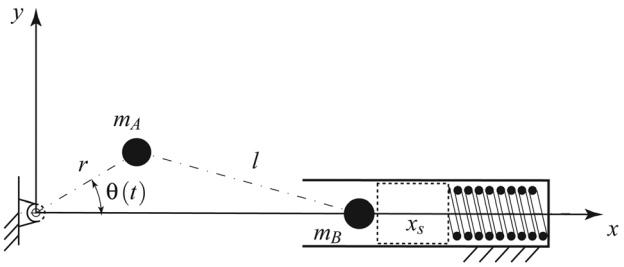

Fig. 3 Slider position and frame of reference

$$M_A = \frac{I_{gr}}{r^2} + \frac{5}{6}m_l + m_s \sin^2\theta + 2\frac{m_s\lambda \sin^2\theta\cos\theta}{\sqrt{1-\lambda^2\sin^2\theta}} + \frac{m_s\lambda^2\cos^2\theta\sin^2\theta}{1-\lambda^2\sin^2\theta} + \frac{1}{6}m_l\sin^2\theta + \frac{m_l\lambda\sin^2\theta\cos\theta}{\sqrt{1-\lambda^2\sin^2\theta}} + \frac{1}{6}\frac{m_l\lambda^2\cos^2\theta\sin^2\theta}{1-\lambda^2\sin^2\theta} + \frac{1}{6}\frac{m_l\cos^2\theta}{1-\lambda^2\sin^2\theta} - \frac{2}{3}m_l\cos^2\theta \quad (1)$$

$$M_B = m_s \quad (2)$$

2.2 Computation of Crank Angular Acceleration. After the application of the principle of virtual work to the scheme of Fig. 3, one obtains

$$\delta W = -m_B\ddot{x}_s\dot{x}_s - m_A\ddot{\theta}r^2\omega - kx_s\dot{x}_s = 0 \quad (3)$$

where the term x_s of the above expression can be analytically computed both using the exact and the approximate expressions as follows:

$$x_s = r\left(\cos\theta + \frac{\sqrt{1-\lambda^2\sin^2\theta}}{\lambda}\right) \quad (4)$$

$$x_s = r\left(\frac{1}{\lambda} - \frac{\lambda}{4}\right) + r\left(\cos\theta + \frac{1}{4}\lambda\cos 2\theta\right) \quad (5)$$

The terms $\dot{x}_s$ and $\ddot{x}_s$ are obtained by taking the first and second derivatives of Eqs. (4) and (5), respectively.

Substituting the computed expressions of x_s, $\dot{x}_s$ and $\ddot{x}_s$ in Eq. (3), simplifying with respect to the virtual angular velocity ω and solving for $\ddot{\theta}$ it is possible to compute the expression of the angular acceleration $\ddot{\theta}(\theta, \omega, \lambda, R_m)$ as a function of the angle θ, the virtual angular velocity ω, the geometric ratio λ and the inertia ratio $R_m = m_A/m_B$.

The goal is to compute the value of the initial angle θ_0 for which the angular acceleration reaches a maximum for different values of the parameters λ and R_m. This will be done for both cases of $\lambda > 1$ and $\lambda < 1$, using Eqs. (4) and (5), respectively.

2.3 The Revolute Joint Friction-Clearance Model. In order to reduce the number of parameters for studying the effects of friction and clearance a very simple bidimensional friction model has been setup. With reference to Fig. 4, two friction coefficients are introduced:

1. the classical Coulomb dynamic friction coefficient f;
2. a joint friction coefficient f_G that directly relates the reaction force at the joint with the braking torque M_b.

The determination of f_G from the value of f can be complicated. For our purpose, we will assume the local friction coefficient independent from the orthogonal load. With reference to Fig. 4, we can write the following equilibrium equations:

$$\begin{aligned} P(\cos\theta + f\sin\theta) &= F \\ P(-\sin\theta + f\cos\theta) &= 0 \\ fRP &= Fl \end{aligned} \quad (6)$$

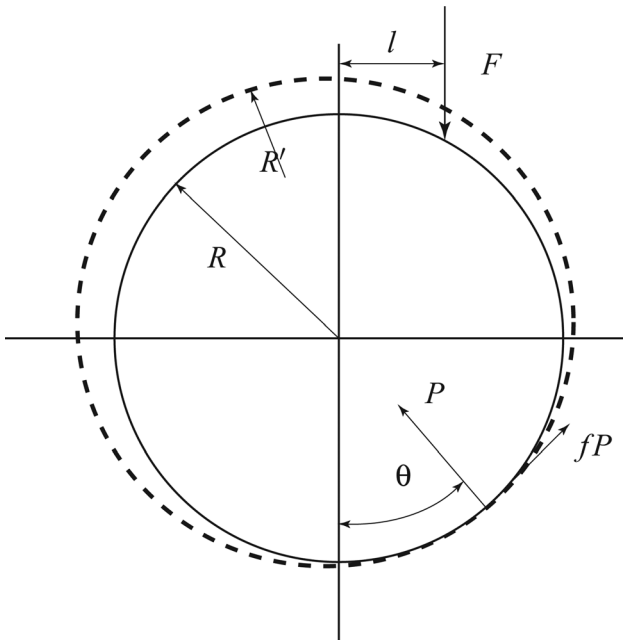

Fig. 4 Planar model of clearance and friction in a cylindrical joint

Solving the system we have

$$\begin{aligned} f &= \tan\theta \\ P &= F/\sqrt{1+f^2} \\ \frac{l}{R} &= \frac{f}{\sqrt{1+f^2}} \end{aligned} \quad (7)$$

The resisting friction generated torque is

$$M_b = FR\frac{f}{\sqrt{1+f^2}} \quad (8)$$

Hence, the joint friction coefficient is herein defined as follows:

$$f_G = \frac{M_b}{FR} = \frac{f}{\sqrt{1+f^2}} = \sin\theta \quad (9)$$

The solution of the problem in presence of friction has to be computed iteratively.

2.4 Helical Spring Dynamic Optimization Process. The optimization procedure herein adopted for the helical spring uses the same criteria of the one proposed by Johnson [14]. According to this methodology, in order to consider both dynamics and structural aspects, two conditions have to be verified:

(1) in designing a helical spring for high speed mechanism, generally the natural frequency f_{n1} should be appreciably greater than any significant Fourier component of the forcing function acting on the spring;
(2) the maximum shear stress, that occurs at the outer fibers (as shown in Fig. 5), must not exceed the admissible value for the material.

These conditions, together with the space limitations constraints and the manufacturing limitations and standards, are adopted for the optimization process. The equations that express the conditions above are, respectively, the followings:[1]

[1]Equations (10) and (11) are valid for A.S. 5 music wire but their deduction procedure is general and can be applied to other materials.

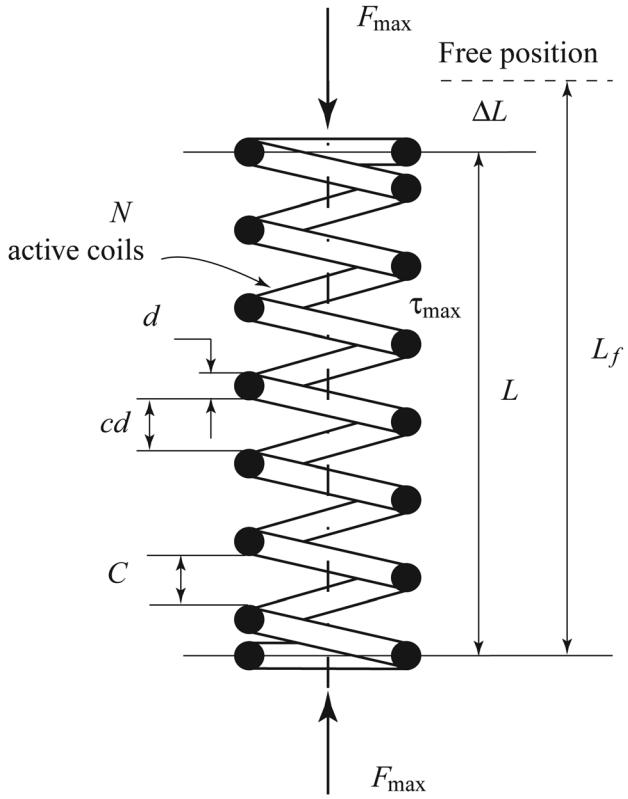

Fig. 5 Helical spring representation and variables for the optimization process

(1) If a choice exists, and if the functional requirements parameters are *not* independent of each other, they should be chosen as to maximize the factor

$$\frac{k^{0.905}}{F_{\max} N_e (1.715 - 0.285\eta)} \tag{10}$$

with $\eta = F_{\min}/F_{\max}$;

(2) Considering the maximum shearing stress theory of fatigue failure [14], this condition must be verified

$$\tau_{\max} d^{0.145} \leq \frac{100000}{(1.715 - 0.285\eta) N_e} \tag{11}$$

During the design process, the parameters have to be chosen as to guarantee the spring to have the required stiffness

$$k = \frac{Gd^4}{8D^3 N_e} \tag{12}$$

The diameter D should be as large as possible, so the space limitation constraints bound the choice of this parameter (remaining in the range of $4 \leq (D/d) \leq 20$). In addition the number of coils N_e should be greater than 3 and the wire diameter d has to be in the range of manufacturing standard.

3 Numerical Results

In this section the general design charts will be reported and commented. Some results on the influence of friction and elasticity of bodies will be shown and the full algorithm for the spring optimization process will be explained and applied to a simple case. A general numerical example with a validation in ABAQUS, both for the mechanism and for the spring, will follow.

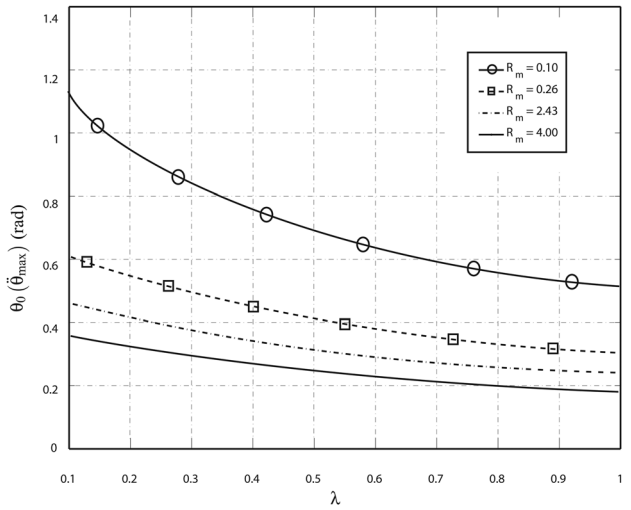

Fig. 6 Initial angle values which corresponds to a maximum value of angular acceleration: case $\lambda < 1$

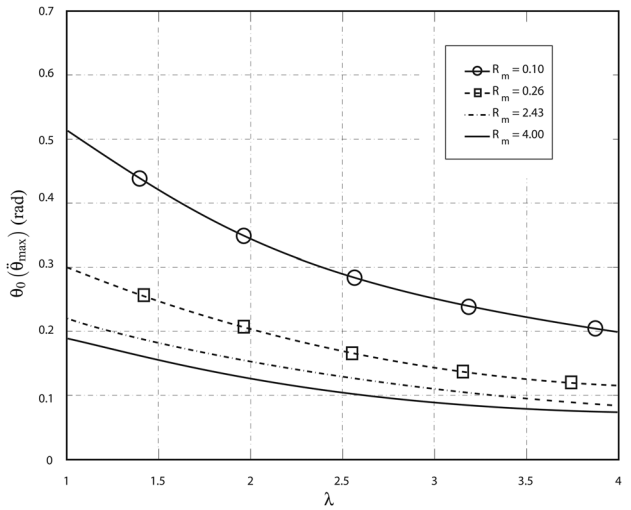

Fig. 7 Initial angle values which corresponds to a maximum value of angular acceleration: case $\lambda > 1$

3.1 General Design Charts. After the procedure described in Sec. 2.2, the design charts have prepared out for both the cases of $\lambda > 1$ and $\lambda < 1$. For the case of $\lambda > 1$, the values of θ which satisfy the following inequality have been excluded for singularity of Eq. (4):

$$\lambda^2 \sin^2 \theta > 1 \tag{13}$$

Figures 6 and 7 report the initial angle θ_0 which corresponds to the maximum value of the angular acceleration $\ddot{\theta}$, function of λ, for different values of R_m. The range of variation of the inertia ratio is $0.1 \leq R_m \leq 4.0$.

From the plots, it is clear that there is a consistent variation of the crank optimal initial position when both the parameters are varying. For the case of $\lambda > 1$, the values of the optimum initial angle are slightly lower than in the case of $\lambda < 1$.[2]

[2]The reader should pay attention to avoid lock–up or bifurcation positions during the deployment phase for the case of $\lambda > 1$.

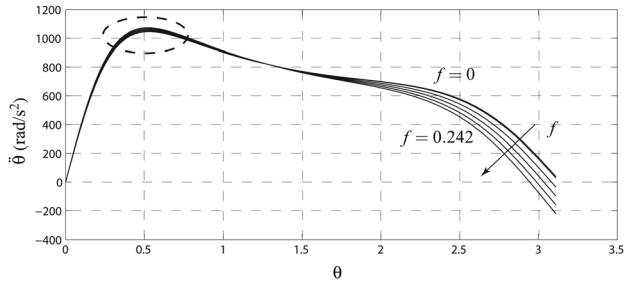

Fig. 8 Influence of friction on the revolute joints: stiffness value $k = 1500$ Nm

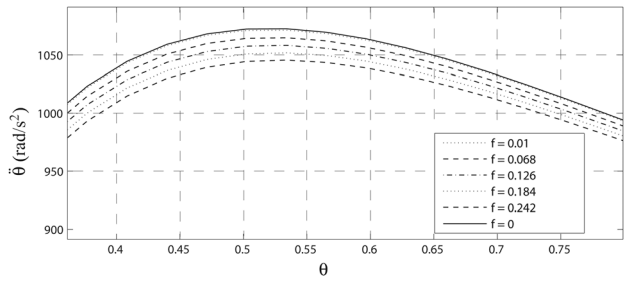

Fig. 9 Influence of friction on the revolute joints: detailed view

3.2 Influence of Friction and Clearance. Herein, the influence of friction and clearance at the revolute joints is analyzed. Only the influence of the variation of the local friction coefficient f for a fixed clearance is discussed. From the executed analysis, the variation of the clearance seems not to have meaningful effects on the deployment time. The relative clearance is defined as $\Delta R/R$ and for this parameter a value $\Delta R/R = 0.002$ is considered as suggested in Ref. [12]. The results herein reported refer to friction added only to the revolute joint between the ground and the crank.

Figure 8 shows the variation of the angular acceleration $\ddot{\theta}$ with the crank angle θ for different values of the local friction coefficient f. The presence of friction affects even the part with higher values of angular acceleration, as shown in the detailed view of Fig. 9.

The results show that the variation introduced in the angular acceleration by the presence of friction reaches 2% for a single revolute joint. For a higher number of revolute joints, there could be the need of taking into account such problem.

3.3 Spring Optimization. The first step in this process is to perform the fast Fourier transform (FFT) of the elastic forcing function acting on the slider Then the frequency values with corresponding amplitudes which are up to 85% of the maximum amplitude value have to be disregarded. The design natural frequency (f_D) for the spring will be the maximum value of the frequency range with increments of 10%. This frequency will be an input for the optimization algorithm which will be a function of the following parameters:

$$(d, D, N_e) = f_{\text{opt}}(f_D, k, D_{\max}, N_{\min}, F_{\max}, F_{\min}) \tag{14}$$

Using the theory outlined in Sec. 2.4, the proposed optimization procedure goes through the following steps:

(1) adopt the $D_{\max}$ as design value ($D = D_{\max}$);
(2) adopt the $N_{\min}$ as design value in order to maximize Eq. (10);
(3) solve the nonlinear over defined system defined by Eqs. (11) and (12) with a least squares method;
(4) modify the value of d adopting a manufacturing standard;
(5) check the value of the new natural frequency and apply the failure theory again.

Table 1 Geometry and inertia for the test problem

Link	m (g)	I_g (g · mm^2)	l (mm)
crank	14.32	2704.55	40
coupler	77.67	45917.36	80
slider	26.40	—	—

Table 2 Spring data and constraints for the test problem

k (N/m)	$D_{\max}$ (mm)	$N_{\min}$
1500	150	3

Table 3 Joint data for the test problem

Property	Value
Joint clearance	0.02 (mm)
Friction coefficient	0.05

Table 4 Results of the optimization procedure for the test problem

θ_0 (rad)	t_{dep} (ms)	N	d (mm)	D (mm)	L_f (mm)
0.5969	16.128	3	4.4	150	43.94

Tables 1–3 provide the data for a test mechanism. In Table 4, the results of the optimization process for that mechanism are shown. The deployment time has been computed by using the approximation of constant angular acceleration $\ddot{\theta} = \ddot{\theta}_{\max}$ for a deployment angle of 20°.

4 Model Validation

The results of the optimization procedure have been validated through the use of a the commercial software ABAQUS. Two analyses have been implemented in order to check for the reliability of the obtained results:

(1) A rigid body dynamics analysis of the slider–crank, with friction on the revolute joint and the spring modeled as a force acting on the system in which we check for the deployment time;
(2) A nonlinear explicit FEM analysis of the spring modeled as a deformable body in which the maximum shear stress inside the spring is verified and also its natural frequency.

Because of the concentrated mass model and of the approximations made through the modeling phase, a slight difference between the deployment time computed by the use of the two methods should be noticed. The value of the percentage error on the computation of the deployment time can be computed with Eq. (15). Its value will increase or decrease depending on the value of the crank angular jerk. An increase of the jerk corresponds to an increase of such error, because of the approximation of constant acceleration in computing the deployment time.

$$E = \left| \frac{t_A - t_S}{t_A} \right| \tag{15}$$

For the specific example discussed in Sec. 3, a deployment time of $t_{\text{dep}} = 17.813$ ms was obtained. This value leads to a percentage error $E_{DT} = 9.46\%$. Repeated tests for 20 different configurations

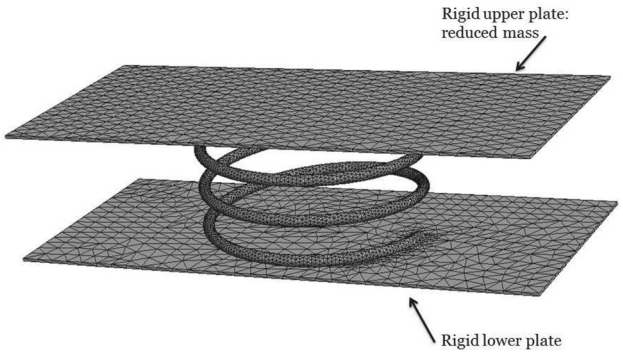

Fig. 10 FE model description

of the mechanism were conducted and the value of the error for each simulation never reaches 10%.

Finally, a FE analysis has been set up with the optimum parameters in order to check for the maximum shear stress value and for the natural frequency. In particular ABAQUS explicit was used to analyze a solid finite element model of the spring. The material used for this simulation is the *Music Wire ASTM A 228* with a Young's modulus of $206842 \cdot 10^6$Pa and a Poisson coefficient $\nu = 0.285$. A compression displacement of 0.022 m has been applied and suddenly removed while a reduced mass has been introduced as a rigid body in order to simulate the inertia of the mechanism as it is shown in Fig. 10.

The value of the equivalent stress computed according to Von Mises theory never reaches critical value as expected. Moreover, for the specific example discussed in Sec. 3, the percentage error on the natural frequency is $E_{NF} = 4.98\%$. Again repeated tests for 20 different configurations of the mechanism were conducted and the error values are always below 6%.

5 Conclusions

In this paper, a general optimization procedure for a first stage conceptual design of a HSD mechanism has been developed and applied to a planar slider–crank mechanism. The design charts were specifically developed and tested for the slider–crank because of its constructive simplicity and multiplicity of use. A dynamic oriented *design charts* approach has been used for the first time in order to find the optimum initial configuration of the system. In order to reduce the number of parameters in the, we operated a lumped mass reduction of the mechanism was used.

The results show a consistent change in the optimal initial position with the variation of the chosen parameters. The effects of friction and clearance at the revolute joints have been also investigated with a simplified iterative model. The results show that it is not possible to neglect these effects, especially when a consistent number of pin joints is used.

Finally, an optimum design of the spring which actuates the mechanism has been performed in order to maximize the natural frequency of the spring. The constrained optimization algorithm takes into account both dynamic and structural features using the maximum shear stress theory as failure criterion.

The results show a good agreement with the one obtained by using commercial software. In particular the deployment time obtained by modeling a rigid bodies slider–crank in ABAQUS, is not much different from the value computed using the approach herein presented. Moreover, a FE analysis has shown that the values of the stress are always lower than the admissible value for the material and the natural frequency is greater than any significant Fourier component of the forcing function acting on the spring.

Important design requirements as reliability and stability have not been considered. Detailed consideration on these topics should be mainly addressed after a detailed design, which is beyond the scope of the present paper. Similarly, no distinction has been made between high and low load cases. The focus of the procedure has been on a quick first dimensioning of the parts, such as the spring, the main mechanism proportions and mass ratios. Further analyses, would require additional data that, in a first design stage, may be not available.

The obtained design charts can be used as a guideline for the design of a planar slider–crank for high speed application. Furthermore, the discussed algorithm has been implemented according to a general methodology and can be easily extended to other planar mechanisms providing actual inertial and geometric data.

Nomenclature

c = percentage clearance between coils on the spring ($C = cd$)
C = absolute clearance between coils on the spring
d = diameter of the spring wire
D = diameter of the spring
E = Young's modulus
E_{DT} = percentage error on deployment time
E_{NF} = percentage error on natural frequency
f = local friction coefficient
F = reaction force at the joint
f_G = joint friction coefficient
$F_{\min}, F_{\max}$ = minimum and maximum value of the force acting on the spring
G = shear modulus
l = coupler length
I_{gl} = coupler baricentric moment of inertia
I_{gr} = Crank baricentric moment of inertia
k = spring stiffness
L_f = free length of the spring
m_A = lumped mass at the top of the crank
m_B = lumped mass at the slider center
m_l = coupler mass
m_r = Crank mass
m_s = slider mass
M_b = breaking friction torque
N_e = number of active coils for the spring
r = Crank length
R = radius of the inner pin of the revolute joint
$R_m = m_A/m_B$ = inertia ratio
t = time
$x_s, \dot{x}_s, \ddot{x}_s$ = slider position, velocity, and acceleration, respectively
δW = virtual work
η = ratio between minimum and maximum value of the force acting on the spring
$\lambda = r/l$ = Crank and coupler link ratio
ω = Crank virtual angular velocity
$\theta(t), \dot{\theta}(t), \ddot{\theta}(t)$ = Crank angular position, speed and acceleration
$\tau_{\max}$ = maximum value of the shear stress

References

[1] Mitsugi, J. E. A., 2000, "Deployment Analysis of Large Space Antenna Using Flexible Multibody Dynamics Simulation," Acta Astron., **47**(1), pp. 19–26.
[2] Dietz, S. E. A., 2003, "Nodal vs. Modal Representation in Flexible Multibody System Dynamics," ECCOMAS Multibody Thematic Conference.
[3] Rossoni, P. E. A., 2004, "Deployment Mechanism for the Space Technology 5 Micro Satellite," Aerospace Mechanism Symposium.
[4] Wallrapp, O., and Wiedemann, S., 1998, "Simulation of Deployment of a Flexible Solar Array," Multibody Syst. Dyn., **2**, pp. 1–24.
[5] Powers, J., Harris, J., Etherton, J., Ronaghi, M., Snyder, K., Lutz, T., and Newbraugh, B., 2001, "Preventing Tractor Rollover Fatalities: Performance of the NIOSH AutoROPS," Injury Prevention.
[6] Powers, J., Harris, J., Etherton, J., Ronaghi, M., Snyder, K., Lutz, T., and Newbraugh, B., 2000, "Performance of an Automatically Deployable ROPS on ASAE Tests," ASAE Annual Meeting.
[7] McKenzie, E., Ronaghi, M., Powers, J., and Lutz, T., 2008, "Implementing and Developing Industry Standards," American Society of Safety Engineers, **6**,

pp. 58–62. Available at: https://www.onepetro.org/conference-paper/ASSE-07-0341
[8] Ravn, P., A., 1998, "A Continuous Analysis Method for Planar Multibody Systems With Joint Clearance," Multibody Syst. Dyn., **2**, pp. 1–24.
[9] Flores, P. A. J., and Pimenta Claro, J., 2004, "Dynamic Analysis for Planar Multibody Mechanical Systems With Lubricated Joints," Multibody Syst. Dyn., **12**, pp. 47–74.
[10] Valentini, P., Stefanelli, R., and Vita, L., 2005, "Modelling of Hydrodynamic Journal Bearing in Spatial Multibody Systems," ASME International Design Engineering Technical Conferences.
[11] Pezzuti, E., Stefanelli, R., Valentini, P., and Vita, L., 2006, "Computer-Aided Simulation and Testing of Spatial Linkages With Joint Mechanical Errors," Int. J. Numer. Methods Eng., **65**, pp. 1735–1748.
[12] Brutti, C., Valentini, P., and Coglitore, G., 2011, "Modeling 3D Revolute Joint With Clearance and Contact Stiffness," Nonlinear Dyn., **66**, pp. 531–548.
[13] Lee, J., and Thompson, D., 2001, "Dynamic Stiffness Formulation, Free Vibration and Wave Motion of Helical Springs," J. Sound Vib., **239**, pp. 237–320.
[14] Johnson, R., 1961, *Optimum Design of Mechanical Elements*, John Wiley & Sons.
[15] Yildirim, V., 1998, "Investigation of Parameters Affecting Free Vibration Frequency of Helical Springs," Int. J. Numer. Methods Eng., **39**, pp. 99–114.
[16] Freudenstein, F., Primrose, E., Ray, S., and Laks, B., 1976, "Velocity Fluctuations in Four-Bar Linkages and Slider-Crank Mechanisms," ASME J. Eng. Indus., **98**(4), pp. 1255–1259.
[17] Dukkipati, R., and Osman, M., 1981, "Velocity Fluctuations in Spatia Slider-Crank Mechanisms," Mech. Mach. Theory, **16**, pp. 487–495.
[18] Freudenstein, F., 1956, "On the Maximum and Minimum Velocities and the Accelerations in Four-Link Mechanism," Trans. ASME, **78**, p. 779.
[19] Wittenbauer, F., 1923, *Graphische Dynamik*, Verlag von Julius Springer, Berlin.